Korean J. Chem. Eng., **31**(11), 2041-2050 (2014)
DOI: 10.1007/s11814-014-0169-1

pISSN: 0256-1115
eISSN: 1975-7220

Gas separation properties of polyvinylchloride (PVC)-silica nanocomposite membrane

Mohammad Mohagheghian*, Morteza Sadeghi,†, Mahdi Pourafshari Chenar*, and Mahdi Naghsh****

*Chemical Engineering Department, Faculty of Engineering, Ferdowsi University of Mashhad, Mashhad 91775-1111, Iran
**Chemical Engineering Department, Isfahan University of Technology, Isfahan 84156-8311, Iran
(*Received 28 February 2014 • accepted 19 June 2014*)

Abstract–Researchers have focused on improving the performance of polymeric membranes through various methods, such as adding inorganic nanoparticles into the matrix of the membranes. In the present study, the separation of oxygen, nitrogen, methane and carbon dioxide gases by PVC/silica nanocomposite membranes was investigated. Silica nanoparticles were prepared via sol-gel method. Membranes were prepared by thermal phase inversion method and characterized using Fourier transform infrared spectroscopy (FTIR), scanning electron microscopy (SEM), differential scanning calorimetry (DSC) and thermal gravimetry (TGA) analyses. The FTIR and SEM analyses demonstrated a nano-scale dispersion and good distribution of silica particles in the polymer matrix. According to TGA results, thermal properties of PVC membranes were improved and DSC analysis showed that glass transition temperature of nanocomposite membranes increased by adding silica particles. We concluded that the permeability of carbon dioxide and oxygen increased significantly (about two times) in the composite PVC/silica membrane (containing 30 wt% silica particles), while that of nitrogen and methane increased only 40 to 60 percent. Introducing 30 wt% silica nanoparticles into the PVC matrix, increased the selectivity of CO_2/CH_4 and CO_2/N_2 from 15.9 and 21 to 18.2 and 27.3, respectively. The diffusion and solubility coefficients were determined by the time lag method. Increasing the silica mass fraction in the membrane increased the diffusion coefficients of gases considered in the current study.

Keywords: Gas Separation, Nanocomposite Membrane, Silica, Polyvinylchloride (PVC)

INTRODUCTION

Membrane-based gas separation processes have become more attractive over traditional technologies in different gas separation and purification processes, such natural gas treating, air separation, olefin/paraffin separation, and hydrogen purification. They offer lower capital and operating costs, lower energy requirements, and ease of operation [1]. The gas separation performance of many polymers has been studied in the literature [2].

Poly(vinyl chloride) (PVC) is a polymer with a wide variety of applications in different industries due to high compatibility with additives, easy process ability and recyclability. Despite the extensive use of PVC in several industrial applications, studies on the gas separation performance of PVC membranes are scarce [3]. Previous studies showed that PVC membrane exhibits low permeability to gases [3-6]. Improvement of the permeability of PVC membranes is studied elsewhere [3-7].

Bierbrauer et al. [3] reported the modification of PVC by partially replacing the chlorine atoms of the chains with moieties derived from fluorinated nucleophilic compounds: 4-fluorothiophenol, 3,4-difluorothiophenol and pentafluorothiophenol. Functionalizing moieties causes significant increase in the permeability of PVC membranes. Tiemblo et al. [5] measured the diffusivity, permeability, and solubility coefficients of O_2, N_2, CO_2, and CH_4 gases in PVC and in four samples of PVC functionalized with mercapto pyridine groups up to 6.8, 11, 21, and 46 mol%. The permeability of all four gases progressively increased by a factor of more than 4 because of a similar increase in the diffusion coefficients. Tiemblo et al. also [6] studied the nucleophilic substitution of chlorine atoms with 4-mercaptophenol sodium salt, 2-thionaphthalene, 4-(1-adamantyl) thiophenol, and thiophenolate sodium salt as the nucleophiles, from low conversion levels (3%) to high levels (40%). The obtained results showed that the introduction of bulky groups into the PVC chain prevents the chain packing and results in large increase in the free volume and permeability at conversions up to 10%. We [7] studied before the effect of the molecular weight of polyethyleneglycol (PEG) on the gas permeability and selectivity of a series of polyvinylchloride/polyethyleneglycol (PVC/PEG) blend membranes. The PVC/PEG blends containing 10, 20, and 30 wt% of PEG4000 showed CO_2 gas permeabilities equal to 0.84, 2.38, and 5.82 Barrer, respectively. Our results showed CO_2/N_2 and CO_2/CH_4 selectivities increased up to 110 and 83, respectively, in PVC/PEG blend membrane containing 30 wt% PEG. Jones et al. [8] used PVC hollow fiber membranes for reliably separating oxygen and ozone gas mixtures.

One of the most important and practical methods for improving the gas separation performance of polymeric membranes is the incorporation of inorganic materials like silica nanoparticles into the polymer matrix. The presence of nanoparticles in the polymer matrix leads to the enhancement of the mechanical strength and thermal stability of the polymer as well as increasing the permeability of nanocomposite membranes [9-11]. In recent years, gas permeation properties of numerous nanocomposite membranes have been studied. The effect of adding silica nanoparticle to polybenzimidazole (PBI) membrane showed that the permeability of CO_2 and its selectivity over N_2 was increased from 0.025 barrer and 3.5 in pure PBI to 0.11 barrer and 71.3 in the nanocomposite containing 20 wt% of

†To whom correspondence should be addressed.
E-mail: m-sadeghi@cc.iut.ac.ir

the silica particles [8]. The H_2 and O_2 permeability of TiO_2/polyimide nanocomposite membrane with TiO_2 content of 25 wt% was reported 3.7 and 4.3 times higher than that of pure polyimide [12]. The addition of MgO nanoparticles to polyimide (Matrimid®5218) led to an increase in gas permeability of membranes; the highest permeability was observed for the membranes containing 40 wt% MgO loading [13]. A significant increase in permeability of CO_2, CH_4 and N_2 gases as well as CO_2/N_2 and CO_2/CH_4 selectivities was observed upon increasing the silica content of EVA membrane [14]. In polysulfone-silica mixed matrix membrane, the O_2 permeability is approximately four-times higher and CH_4 permeability is over five-times greater than in a pure PSf membrane [15]. Adding mesoporous silica spheres to polyimide Matrimid® membrane improved gas permeability [16].

The results of previous research showed that the permeability of gases through PVC membranes is low and it should improve. As mentioned, we tried to enhance gas separation properties of PVC by PEG before [7]. As studied by this group and reported in literature, adding silica nanoparticle has good effect in permeability and gas separation performance of polymeric membranes. Considering the advantages of PVC membranes, this membrane could be used as hollow fiber membrane by improving their permeability. So, in this research, we tried to enhance the gas permeation properties of PVC membrane by addition of silica nano-particles. Silica nanoparticles were prepared via hydrolysis of tetraethoxysilane (TEOS) and membranes were prepared by the solution-casting method.

EXPERIMENTAL

1. Materials

Polyvinylchloride powder was obtained from Vinytai Co., Thailand (K-value: 65-67 and specific viscosity: 0.36-0.38). Analytical grade Dimethylformamid (DMF) solvent, tetraetoxysilane (TEOS), 3-glycidyloxypropylterimethoxysilane (GOTMS), HCL and ethanol, required for preparation of silica nanoparticles, were purchased from Merck with more than 99% purity. The research grade CO_2, O_2, N_2 gases (purity>99.99%) were purchased from Ardestan gas Co., Iran and also CH_4 (purity>99.95%) was purchased from Technical Gas Service.

2. Preparation of PVC Membrane

The PVC solution (8-10 wt% of polymer) was prepared by dissolving PVC powder in (DMF) at 40 °C under agitation. The prepared transparent solution was filtered via a 100-micron filter before casting. The PVC films were cast by casting knife on clean glass sheets. The films remained at 60 °C for 24 hours without any cover in an oven. Finally, the membranes were dried in a vacuum oven at 65 °C for 12 hours to remove the solvent completely. The thickness of prepared membranes was about 35 microns.

3. Preparation of Silica Nanoparticles and PVC-silica Nanocomposite Membranes

Silica nanoparticles were prepared through the sol-gel process via the hydrolysis of TEOS in ethanol in the presence of HCl as described elsewhere [8]. PVC-silica nanocomposite membranes were prepared by addition of silica-sol in different weight fractions into the polymer solution. Solutions containing 5, 10, 15, 20 and 30 wt% of silica nanoparticles were prepared and then filtered via a 100-micron filter before casting. The PVC-silica films were cast by casting knife on clean glass sheets. The films remained at 60 °C for 24 hours without any cover in an oven. Finally, the membranes were dried in a vacuum oven at 65 °C for 12 hours to remove residual solvent completely as well as removing the probable adsorbed water in the membranes.

Table 1. Sample name of prepared membranes and their silica content

Sample name	Silica content (wt%)
PVC	0
PVC- 5S	5
PVC-10S	10
PVC-15S	15
PVC-20S	20
PVC-30S	30

The prepared PVC-silica nanocomposite membranes are named as mentioned in Table 1.

4. Characterization

4-1. FTIR Spectroscopy

Fourier transform infrared spectroscopy (FTIR) in the range of 400-4,000 cm^{-1} (JASCO FT/IR-680 plus) was used to characterize the presence of silica particles in nanocomposite membranes.

4-2. Scanning Electron Microscopy

The morphology of membranes and the presence of nanoparticles in the membranes were determined using scanning electron microscopy (SEM, Philips, XL30) images. For this purpose and in first stage, membranes were immersed in liquid nitrogen and then cooled and broken. The resulting membrane samples were coated with gold on the metallic stubs.

4-3. Thermal Analysis

Thermal properties of the membranes were determined by differential scanning calorimetry (DSC) in the range of ambient temperature to 300 °C at the rate of 10 °C/min (DSC- Netzsch-200 F3 Maia). The thermal degradation of pure PVC and nanocomposite membranes was investigated by thermal gravimetric analysis (TGA) (TGA-50 SHIMADZU, Japan). The sample was heated from the ambient temperature to 600 °C at a rate of 10 °C/min.

4-4. Gas Permeability Measurement

The pure gas (N_2, O_2, CH_4 and CO_2) transport properties of prepared membranes were determined using a constant volume/variable pressure method as described in detail by Pye et al. [17]. The feed side gas pressure was 10 bar (gauge) and the active area of the membrane cell was 13.1 cm^2. The specifications of the constant volume/variable pressure setup are also described in detail elsewhere [18].

The gas permeability of membranes was calculated using the following equation:

$$P = \frac{273.15LV}{76p_0AT}\frac{dp(t)}{dt}$$

where P is the permeability in barrer (1 barrer=1×10^{10} cm^3 (STP) cm/cm^2 s cmHg), V, the volume of the down-stream chamber (cm^3), A, the effective membrane area (cm^2), L, the membrane thickness (cm), T, the experimental temperature (K), dp(t)/dt, the steady rate of pressure measured by a pressure transducer in the down-stream chamber and p_0, the feed pressure with the same unit of p(t). The

diffusion coefficient (D) was calculated by the time-lag method as below:

$$D = \frac{L^2}{6\theta}$$

where θ is the time lag (s), the intercept obtained from extrapolating the linear region of the p(t) versus the time plot to the time axis

D is the diffusion coefficient (cm^2/s).

The solubility coefficient (S) (cm^3 (STP)/cm^3cmHg) was calculated as:

$$S = \frac{P}{D}$$

The ideal selectivity of membranes ($\alpha_{A/B}$) was determined from pure gas permeability as follow:

$$\alpha_{A/B} = \frac{P_A}{P_B}$$

RESULTS AND DISCUSSION

1. Membrane Characterization

1-1. FTIR Spectroscopy

Fig. 1 shows the FTIR spectra of pure polymer, prepared nanocomposite membranes, and pure silica nanoparticles. It is obvious, according to the emerged absorption peaks related to the silica nanoparticles in FTIR analysis, that the hydrolysis of TEOS has been completed and SiO_2 has been formed [19]. The strong peak at the range of 1,077 cm^{-1} indicates the formation of Si-O-Si asymmetric stretching bonds.

The effect of Si-O-Si asymmetric stretching bonds at 1,077 cm^{-1} and 794 cm^{-1} on the spectra of nanocomposite membranes can be observed. As shown in Fig. 2, the peaks related to the bonds Si-O-Si and Si-OH were observed in wave numbers 435, 1,077, and 3,438 cm^{-1}. This figure shows the effect of the silica particles on the absorption of FTIR spectra of polyvinylchloride/silica nanocomposite membrane.

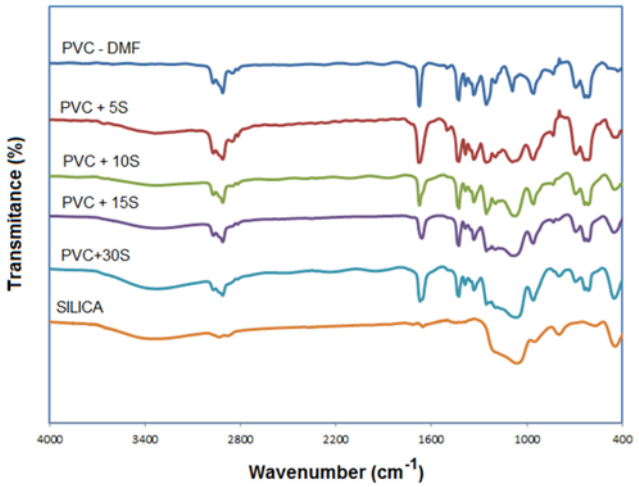

Fig. 1. FTIR spectra of prepared membranes and silica nanoparticles.

1-2. Scanning Electron Microscope (SEM)

The morphology of the membrane affects its permeation properties. SEM images can reveal the morphological properties of the membranes to a great part. The SEM micrographs of the cross-section of the nanocomposite membranes are shown in Figs. 3, 4 and 5 with magnification of 1,000, 30,000 and 60,000, respectively.

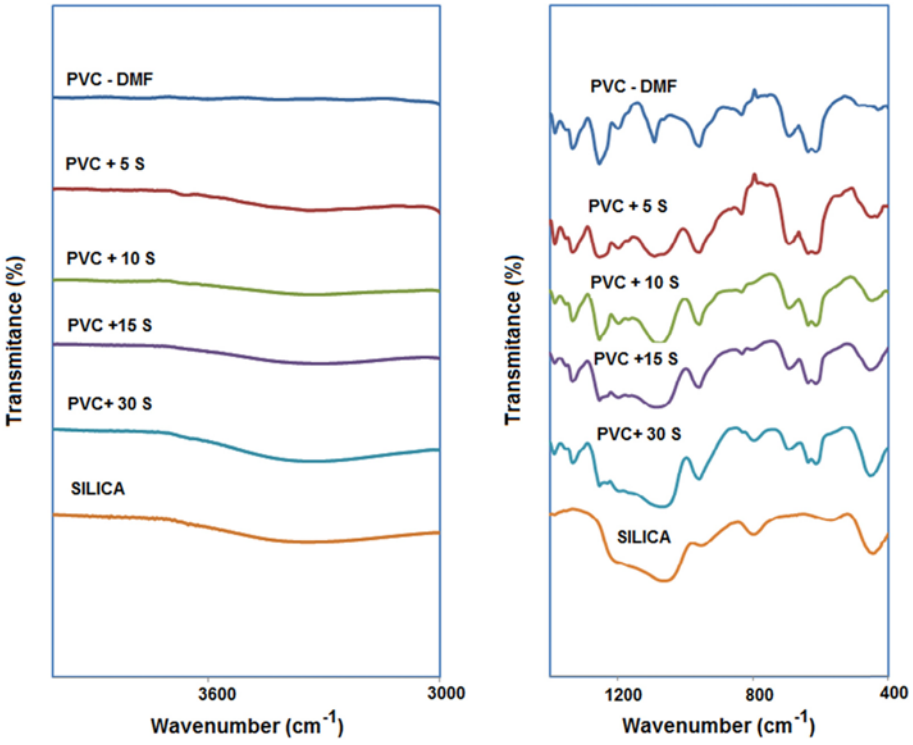

Fig. 2. The effect of the silica particles on the absorption of FTIR spectra of polyvinylchloride/silica nanocomposite membrane.

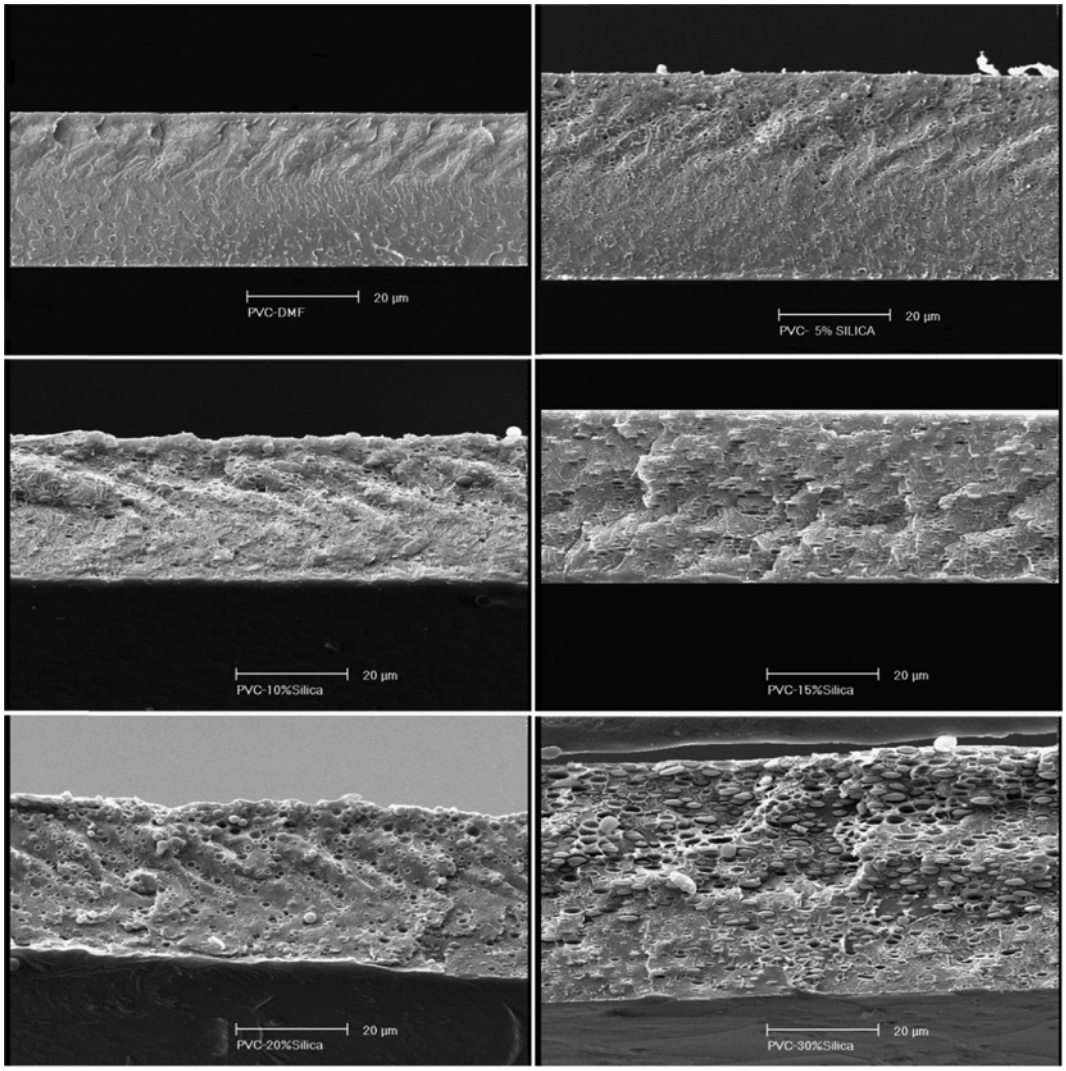

Fig. 3. SEM images of cross section of prepared membranes at a magnification of 1,000.

Fig. 3 reveals that the structure of the pure PVC membrane is quite compact and dense, and the surface roughness of the membrane becomes coarser by increasing the nanoparticles in the polymer matrix. As shown in Fig. 3, nanoparticles become more congregated and agglomerated in the polymer matrix by increasing the weight fraction of silica nanoparticles in the polymer matrix. The structure of polymer network has changed because of the changes at the interface of polymer and silica inorganic phase. Free spaces have been created at the polymer-agglomerated particles. While, according to Figs. 4 and 5 the nano-dispersed silica particles have good connection to the polymer matrix. So, two morphologies have appeared in PVC-silica nanocomposite membranes. The first one is agglomerated silica particles at size about 500 nm, which have poor connection to polymer matrix and free spaces at the interface. The second one, nanodispersed silica nanoparticles at size about 50-70 nm with excellent connection to polymer matrix and any free spaces at interface. In spite of hollow spaces at the interface of polymer-agglomerated particles in the prepared membranes, the presence of nanoscale dispersed silica, providing enough integrity in membranes, makes them tolerate easily the pressure of 10 barg due to the uniform distribution of nanoparticles in the polymer matrix and the compatibility of PVC polymer with silica nanoparticles.

The SEM images of nanocomposite membranes with magnification of 30,000 and 60,000 can be seen in Figs. 4 and 5, respectively. As mentioned earlier, the nanodispersed silica exists in membrane. It is clear that further silica agglomerations are produced and seen by increasing the silica weight fraction in polymer. A split and separation is well observed between the silica particles and polymer at the intersection of agglomerated particles and polymer in Figs. 3, 4 and 5. This behavior can account for a group of silica particles which could not communicate with the coupling agent in the sol-gel process, so reduced their contact surface with the polymer by being agglomerated, and finally the agglomerated particles could not attach to the polymer; and this gap between the particles and the polymer can be observed in the images with further magnification.

Contrary to the silica agglomerations which did not connect very well to the polymer, it is seen that nanometric-size distributed particles connected very well to the polymer matrix and no gap or separation is seen between the particles and the polymer.

Thus, there can be seen two types of morphology for the pro-

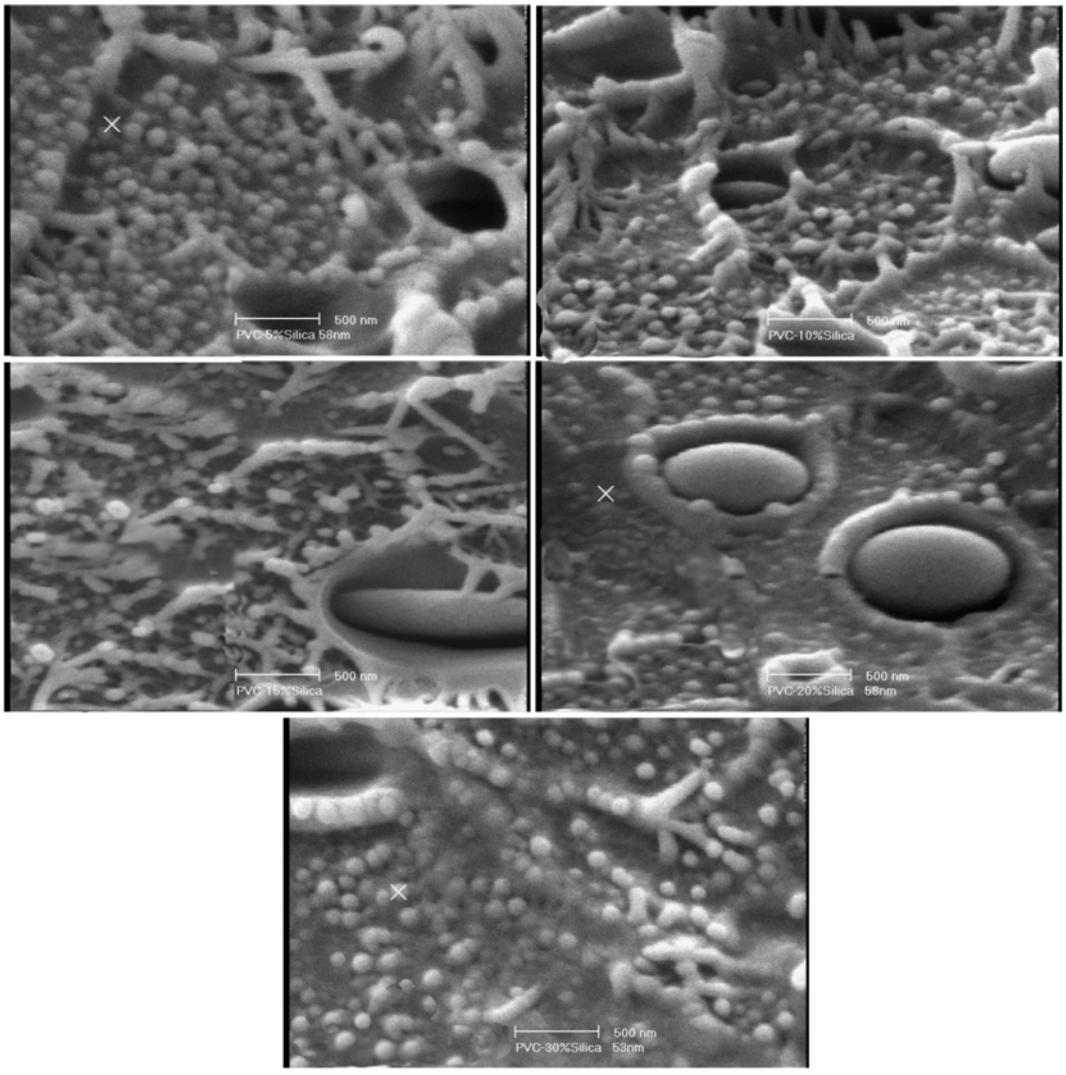

Fig. 4. SEM images of cross section of prepared membranes at a magnification of 30,000.

duced nanocomposites:

1) Micron size distribution of silica particles in the polymer matrix with the weak bonds of polymer-silica, leading to create free space at the interface of polymer and silica.

2) Nanometric distribution of silica particles in the polymer matrix, leading to strong bonds between the particles and polymer matrix.

2. Differential Scanning Calorimetry (DSC)

DSC experiments were carried out to determine glass transition temperature (T_g) of prepared nanocomposites. T_g is a criterion for adjusting the rigidity of polymeric chains. The achieved quantities of T_g for a variety of samples are shown in Table 2. It can be seen that an increase in the weight fraction of silica particles in the membranes increases T_g.

The FTIR spectra and SEM analyses reveal the effective presence of silica particles in polymeric matrix. Moreover, SEM images illustrated that many silica nanoparticles were distributed over the polymeric matrix, and there is a robust bond between the particles and the polymer. The mobility of mineral silica particles is less than polymeric chains, while their rigidity is higher.

Thus, with connecting the silica particles to the polymeric chain, the mobility of the polymeric chain will be reduced resulting in reduction in T_g of polymer. Furthermore, strong interaction between silica particles and polymer chain (As can be seen in SEM images) leads to solidification of chains at polymer/nanoparticle interface and therefore, free-volume of polymer, in this area, will be decreased [19].

The robust connection between silica nanoparticles and polymeric chain had a remarkable effect on the mobility of the polymeric chain. Hence, notwithstanding increasing the free-volume around the micro particles, the diminution of chain mobility has been dominant and caused the rise in T_g of polymer.

3. Results of Thermal Gravimetric Analysis (TGA)

To determine the weight fraction of inorganic materials in the composite membranes and their effects on the thermal stability of polymer, a thermal gravimetric analysis was conducted on the membrane. The analysis indicates the rate of reduction in the weight of sample by the increase in the temperature. As shown in Fig. 6, the sample weight of pure polyvinylchloride approached zero in the temperature of 600 °C. By increasing the silica mass fraction in the membranes, the weight of remaining sample will increase proportional to the silica mass fraction. The graph in Fig. 6 is divided into

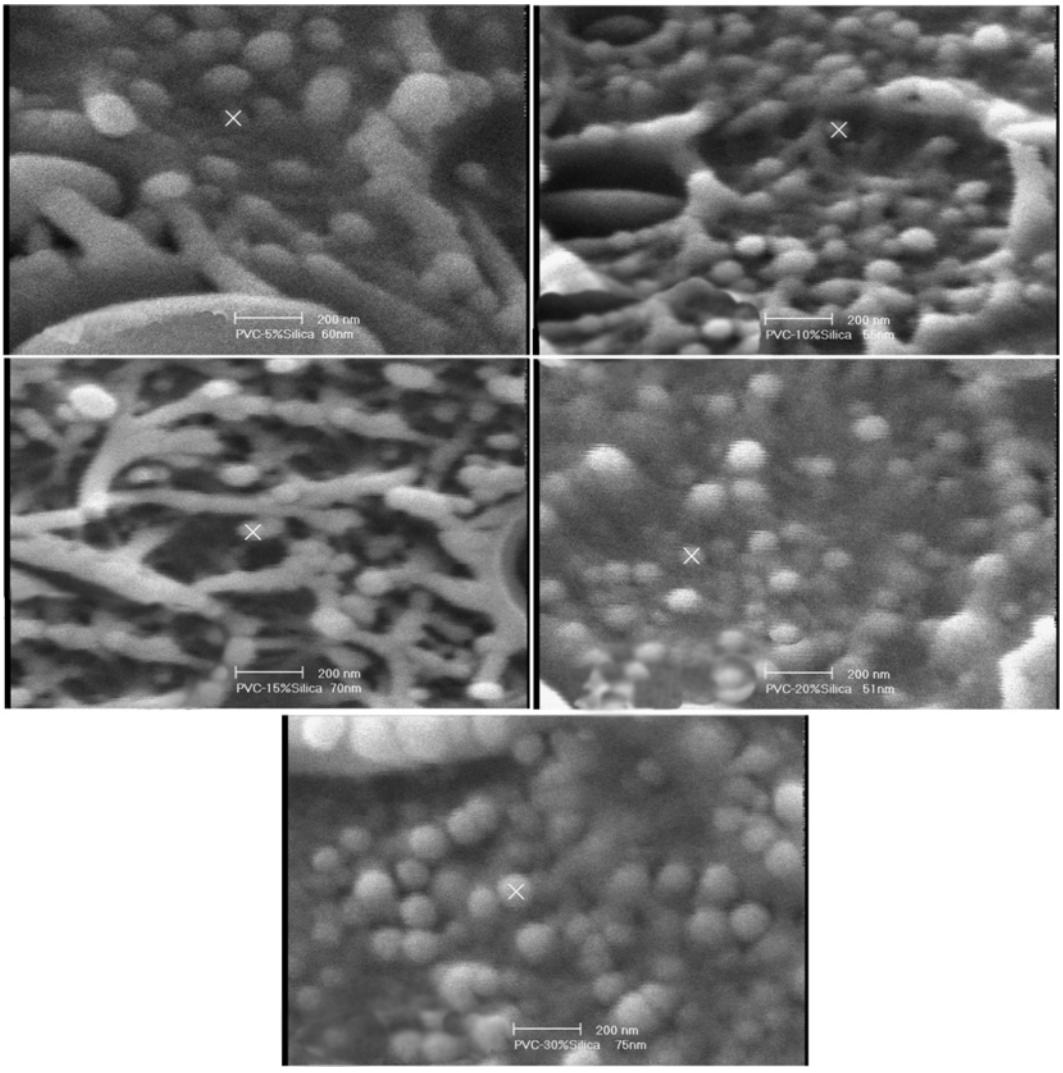

Fig. 5. SEM images of cross section of prepared membranes at a magnification 60,000.

Table 2. The T_g of the membrane samples investigated by DSC analysis

Membrane	T_g (°C)
PVC-DMF	77.0
PVC- 5S	78.8
PVC-10S	81.0
PVC-20S	81.3
PVC-30S	83.7

four parts: the first part consists of the temperatures up to 100 °C at which the volatile materials and the absorbed water by the membranes are removed. The second part includes the temperatures of 100 °C to 250 °C at which corresponding to the removal of remained solvent in the membrane. The third part comprises the temperature range of 250 °C to 350 °C at which the PVC polymer chains are degenerated thermally. The fourth part contains the temperatures over 450 °C at which the materials are carbonized and turn into the ashes [20,21].

In the first and second parts of C 6, temperatures up to 150 °C,

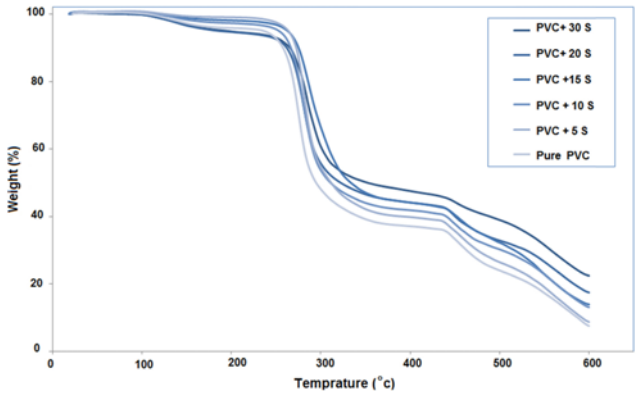

Fig. 6. Thermal degradation of prepared membranes.

the sample weight decreased slightly (about 2 to 4 wt%) indicating small amounts of solvent, water, and volatile materials in the membrane and hence these parameters can be removed from the experiments. Also, it can be found out from the graphs in Fig. 6 that the silica particles slow down the slope of the PVC degeneration in the

third part and consequently improve the thermal resistance of PVC slightly. The inorganic materials require more heat to be turned into the ash than the polymer; as a result, it was expected more material to be left by increasing the silica particles in the membrane structure. The fourth part of the graphs of Fig. 6 indicates this issue very well.

4. Gas Permeation Properties of PVC-silica Nanocomposite Membranes

4-1. Permeability and Selectivity of Pure Gases through the Membranes

The permeability of pure nitrogen, oxygen, methane and carbon dioxide gases was measured on the pure polymer and nanocomposite membranes of polyvinylchloride/silica at 10 barg and 25 °C. The results are given in Figs. 7 and 8.

Fig. 7 shows that the order of permeability of gases in both pure and composite membranes is as follows:

$$P_{CH4}<P_{N2}<P_{O2}<P_{CO2}$$

As known, permeation of molecules through polymeric membranes occurs via solution-diffusion mechanism [7]. Considering that PVC polymer is a glassy polymer, the process of gas separation on this polymer is performed based on domination of diffusion mechanism which can described as molecular sieving. Table 3 reveals the investigations on the kinetic diameter of the relevant gases that the kinetic diameter of studied gases changes as follows:

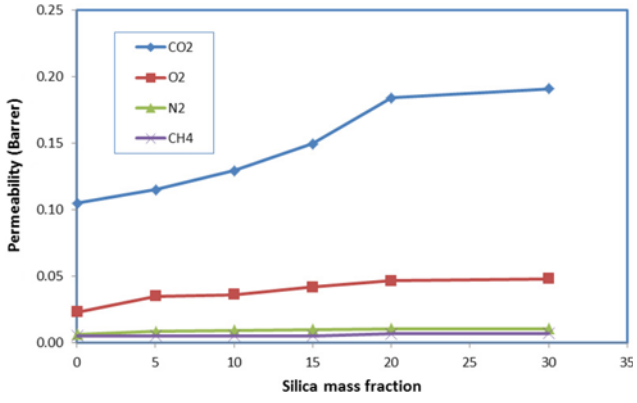

Fig. 7. Gas permeability of membranes at 25 °C and the feed pressure of 10 barg.

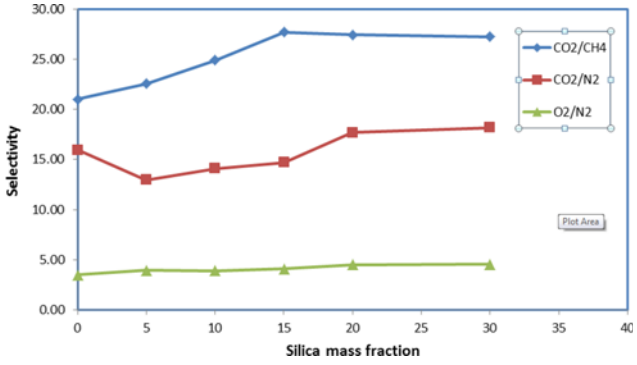

Fig. 8. CO_2/N_2, CO_2/CH_4 and O_2/N_2 ideal selectivities of prepared nanocomposite membranes.

Table 3. The kinetic diameter and condensability of the relevant gases [22]

Gas	Condensability temperature (K)	Kinetic diameter (Å)
CO_2	195	3.30
O_2	107	3.46
N_2	71	3.64
CH_4	149	3.80

$$d_{CO2}<d_{O2}<d_{N2}<d_{CH4}$$

The order of permeability of gases is exactly contrary to the kinetic diameters of studied gases. So, it was found that diffusion is the dominant mechanism in permeability of gases through the polyvinylchloride and polyvinylchloride/silica membranes, and the gases with smaller molecular size have the higher permeability in the membranes.

As shown in Fig. 7, the permeability of gases increased in the membranes by silica particles in PVC. The permeability of carbon dioxide, methane, oxygen, and nitrogen increased from 0.105, 0.005, 0.023, and 0.0066 barrer in pure polymer to 0.1908, 0.007, 0.048, and 0.0105 barrer, respectively, in polyvinylchloride/silica nanocomposite membranes containing 30 wt% silica nanoparticles.

In general, the permeability of gases increases by the following order:

$$P_{CH4}\,(40\%)<P_{N2}\,(59\%)<P_{CO2}\,(82\%)<P_{O2}\,(108\%)$$

As observed in the SEM image, the presence of silica particles results in two groups of particles. The first group consists of micro-size particles which have a weak interaction with the polymer matrix and their contacting surface with the polymer matrix is also weak; it creates a free space at the intersection of particles and polymer. The second group includes the nanoparticles with a good interaction with the polymer matrix and good bonds with the polymer chains. The free space created in the intersection between polymer and micro silica can provide the space needed for the movement of gas molecules in polymer matrix, and it provides more opportunities for transportation of gas molecules through the membrane. Therefore, the permeability increases by silica content of PVC/silica membranes.

Considerable increase in the permeability of carbon dioxide in comparison to other gases is related to structural changes occurring in the membranes. Such changes result from the presence of silica nanoparticles in the polymer matrix, leading to changes in the diffusion and solubility coefficient of gases in the polymer matrix. In the following, the reasons for such changes are investigated, stating the diffusion and solubility coefficients.

Moreover, the increase in the free space enclosed by the polymer provides more suitable space for smaller gases to pass resulting in more increase in the permeability of smaller molecules.

As shown in Fig. 3, the prepared membranes have dense structure with distributed nano-spaces in the polymer-particle interfaces. As a result, gas separation occurs based on solution-diffusion mechanism. Albo et al. showed that in thin film membranes with nano space pores, Knudsen diffusion can contribute effectively in permeation of gases through membrane due to the presence of open pores in membrane structure [30].

Fig. 8 shows the increment in selectivity of studied gases in nano-

Table 4. The solubility and diffusion selectivity for different gases at 25 °C and the feed pressure of 10 barg

Membrane sample	Diffusivity selectivity			Solubility selectivity		
	D_{O_2}/D_{N_2}	D_{CO_2}/D_{N_2}	D_{CO_2}/D_{CH_4}	S_{O_2}/S_{N_2}	S_{CO_2}/S_{N_2}	S_{CO_2}/S_{CH_4}
PVC-30S	3.0	1.1	2.8	1.5	16.8	9.9
PVC-20S	3.0	1.1	3.0	1.5	15.9	9.3
PVC-15S	3.0	1.1	2.8	1.4	13.8	9.9
PVC-10S	3.0	1.2	2.7	1.3	12.0	9.1
PVC-5S	2.9	1.1	2.7	1.4	12.0	8.4
Pure PVC	2.5	1.5	2.9	1.4	10.3	7.4

composite membranes by silica. The selectivity of CO_2/N_2, CO_2/CH_4 and O_2/N_2 increases from 15.9, 21 and 3.5 to 18.2, 27.3 and 4.6, respectively, in nanocomposite membranes containing 30 wt% silica particle. As reported in the SEM analysis, addition of silica nanoparticles in polymer creates some free spaces at the polymer-agglomerated particles. These free spaces would enhance the diffusion and solution of gases in polymer. As reported in Table 4, by addition of silica nano particles to polymer the solubility selectivity of pair gases changes more than diffusivity selectivity. It is due to spaces created in the polymer-agglomerated silica interface which enhance the higher sorption of small gases in comparison to others and finally lead to higher gas selectivity in polymer. Also, the results in Fig. 8 indicate the higher increment in the selectivity of CO_2/N_2 and CO_2/CH_4 pair gases compared to that of O_2/N_2. It is because of the increase in the solubility selectivity of carbon dioxide compared to nitrogen and methane, which will be discussed in the section dealing with the solubility coefficients.

To evaluate the effect of silica nanoparticles in enhancing gas separation properties of PVC-silica membranes, the obtained results were compared with Robeson upper bound and the previous work on PVC-PEG blend membranes [31]. As shown in Fig. 9, silica can enhance the gas separation properties of PVC-silica in CO_2/CH_4 separation, but the PVC-PEG membranes perform better in this separation.

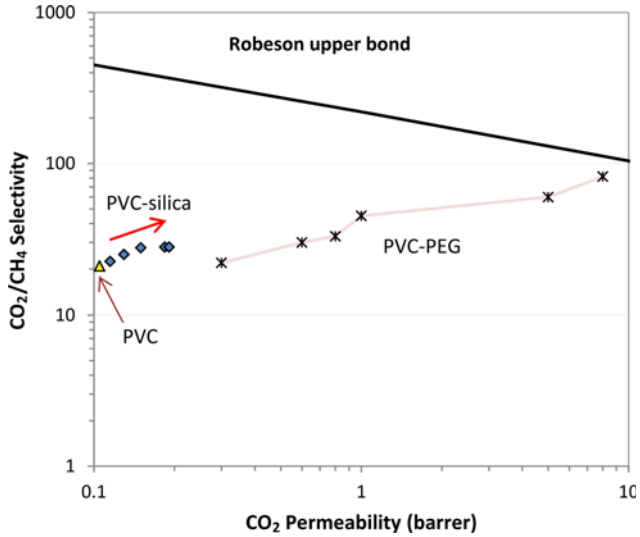

Fig. 9. CO_2/CH_4 separation performance of prepared membranes in comparison to Robeson upper bond.

4-2. Effect of Adding Silica Nanoparticles on Diffusion and Solubility Coefficients of Gases

4-2-1. Diffusion Coefficient

Fig. 10 shows the diffusion coefficient of different gases in the nanocomposite membranes. This figure indicates that the diffusion coefficients of all gases increase by the silica in the nanocomposite membranes.

Also, it is clear that the changes in the diffusion coefficient of gases in pure polymer and nanocomposite membranes are as follows:

$$D_{CH4}<D_{N2}<D_{CO2}<D_{O2}$$

As it is obvious, the diffusion into the polymer is characterized by the molecular size, which is in turn determined by the kinetic diameter. The kinetic diameter is calculated only by the minimum diameter of the molecule profile and only indicates the minimum diameter needed for molecule to penetrate without considering the length of penetrating molecule. So, the diameter establishes a suitable relation with the penetration rate of the short molecules such as gas molecules including oxygen, nitrogen, and methane. Based on the diffusion theory, a gas molecule can penetrate when Brownian movement of the polymer chains provides enough space. This required space depends on the minimum cross-section and the length of penetrating molecule. This can serve as a reason for the linear relation between log D and the kinetic diameter of gas molecules, shown in Fig. 11 for pure PVC and nanocomposite membranes.

As shown in Fig. 11, carbon dioxide does not behave like other gases, and unlike what is expected for oxygen, its permeability does

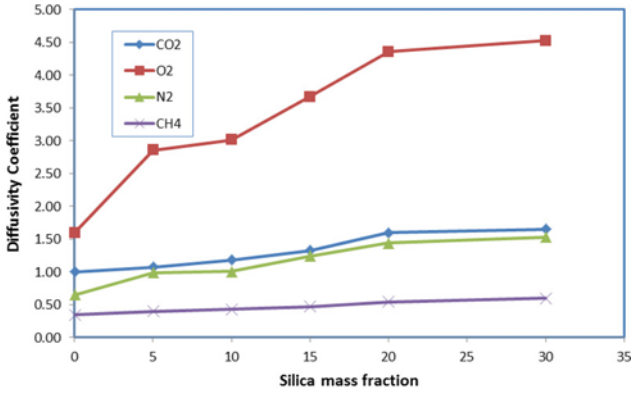

Fig. 10. Diffusion coefficient ($D*10^9$ cm^2/sec) of various gases in nanocomposite membranes at 25 °C and the feed pressure of 10 barg.

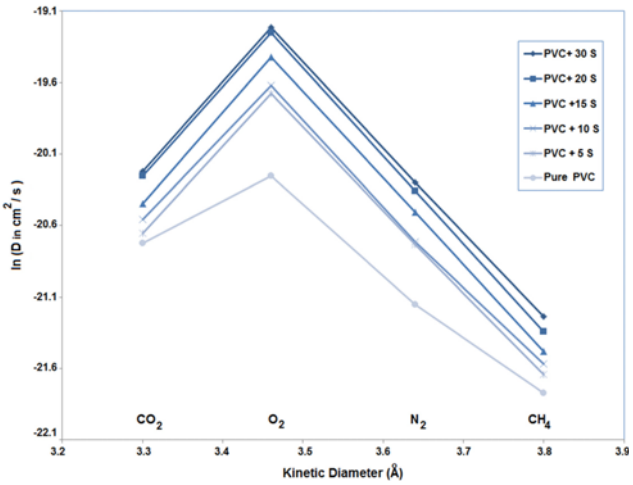

Fig. 11. Correlation of diffusion coefficients to kinetic diameter of gases in composite membranes.

not decrease with the reduction in the kinetic diameter. This can be because the carbon dioxide molecule is non-spherical and it has the double bond in its structure that prevents it from penetrating through the membrane [3].

4-2-2. Solubility Coefficients

As it is clear, the gas sorption in polymeric membranes depends on the condensability of gases, interaction between the polymer and gas molecules, the structure of the polymer, temperature and pressure [8,23-26]. The presence of an electron cloud on the double bond of carbon dioxide results in the increase in the instant bipolarity, and consequently better interaction of this molecule with polymer bonds. In addition to the above-mentioned reasons, it is easier for carbon dioxide to enter the free volumes in the polymer structure because of its smaller molecular size.

Fig. 12 shows the changes in the solubility coefficient of various gases in nanocomposite membranes. Considering above and the results given in Fig. 12, the order for solubility coefficient in the investigated membranes is as follows:

$$S_{CO2}>S_{CH4}>S_{O2}>S_{N2}$$

According to the obtained results, the solubility of gases increases based on their condensability. The presence of silica particles results

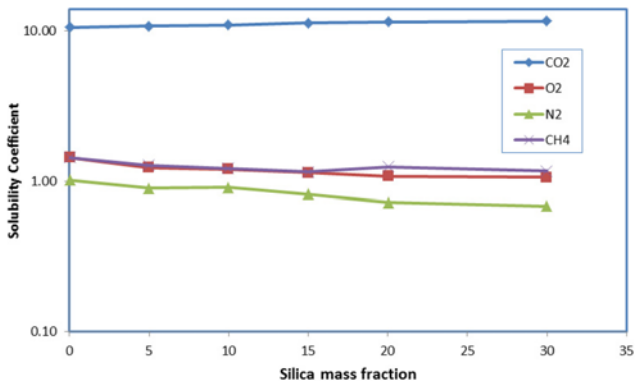

Fig. 12. Solubility coefficient of various gases in membranes at 25 °C and the feed pressure of 10 barg.

in the increase in the density of polar groups of OH in the polymer matrix, and consequently in the establishment of the polar spaces at the intersection of the particles and the polymer. Polar spaces result in an increase in the solubility coefficient of condensable gases [27-29].

The solubility coefficient of carbon dioxide increases more than that of methane because of its polarity, and as a result, the possibility of formation of polar bonds with the polar groups. Table 4 shows the solubility and diffusion selectivity for different gases at 25 °C and the feed pressure of 10 barg.

Considering Table 4, after adding silica nanoparticles, the solubility selectivity as well as its effect on the ideal selectivity will increase because of the increase in the solubility coefficient of carbon dioxide.

CONCLUSIONS

The prepared polyvinylchloride/silica nanocomposite membranes were characterized by the FTIR, SEM, DSC, and TGA tests. The results indicated that the silica nanoparticles synthesized by the sol-gel method were compatible with the polyvinylchloride polymer and were distributed uniformly in the membrane. Also, the presence of nanoparticles improved the thermal properties and also increased the glass transition temperature of the nanocomposite membranes.

Measuring the permeability of pure polyvinylchloride membrane and polyvinylchloride/silica nanocomposite membranes by the constant volume-variable pressure method indicated that the general trend in the permeability in all membranes was as follows, which described the separation and sieving based on the gas molecular size:

$$P(CO_2)>P(O_2)>P(N_2)>P(CH_4)$$

The permeability of gases increases because of the creation of free spaces at the interface of the polymer-silica in the structure of polyvinylchloride. In general, the increase in the permeability of the gases was as follows:

$$P_{CH4}(40\%)-P_{N2}(59\%)-P_{O2}(108\%)-P_{CO2}(82\%)$$

Adding silica nanoparticles into the polyvinylchloride matrix, improved the separation performance of carbon dioxide/methane and carbon dioxide/nitrogen gases. The highest selectivity for carbon dioxide/methane was 27.7 in the membranes containing 15 wt% of silica, and the highest selectivity for carbon dioxide/nitrogen and for oxygen/nitrogen were 18.2 and 4.6, respectively, in the membranes containing 30 wt% of silica.

The order of the diffusion coefficients of gases was as follows by measuring the diffusion coefficients for the studied gases through the time lag method:

$$D_{CH4}<D_{N2}<D_{CO2}<D_{O2}$$

The diffusion coefficient for all gases, except for carbon dioxide, in all the membranes was proportional to the kinetic diameter.

To determine the solubility coefficients of gases, the permeability coefficients were divided by the diffusion coefficients. The order of the solubility coefficients of gases in the studied membranes was as follows, indicating that solubility of gases was increasing based on their condensability:

$S_{CO2}>S_{CH4}>S_{O2}>S_{N2}$

The presence of silica particles resulted in the increase in the density of the polar OH groups in the polymer matrix, and consequently, the establishment of the polar spaces at the intersection of the particles with the polymer. The establishment of the polar spaces increases the solubility coefficient of carbon dioxide because of its polarity.

REFERENCES

1. A. Javaid, *Chem. Eng. J*., **112**, 219 (2005).
2. L. M. Robeson, *J. Membr. Sci*., **320**, 390 (2008).
3. K. Bierbrauer, M. L. Gonzalez, E. Riande and C. Mijangos, *J. Membr. Sci*., **362**, 164 (2010).
4. P. Tiemblo, J. Guzmn, Riande, C. Mijangos and H. Reinecke, *Polymer*, **42**, 4817 (2001).
5. P. Tiemblo, J. Guzmn, E. Riande, C. Mijangos and H. Reinecke, *Macromolecules*, **35**, 420 (2002).
6. P. Tiemblo, J. Guzmn, E. Riande, C. Mijangos, M. Herrero, J. Espeso and H. Reinecke, *J. Polym. Sci., Part B: Polym. Phys*., **40**, 964 (2002).
7. M. Sadeghi, M. Pourafshari Chenar, S. Moradi and M. Rahimian, *J. Appl. Polym. Sci*., **110**, 1093 (2008).
8. C. A. Jones, S. A. Gordeyev and S. J. Shilton, *Polymer*, **52**, 901, (2011).
9. A. Jomekian, S. A. A. Mansoori, N. Monirimanesh and A. Shafiee, *Korean J. Chem. Eng*., **28**, 2069 (2011).
10. A. Laeeq Khan, C. Klaysom, A. Gahlaut, A. Ullah Khan and F. J. Vankelecom, *J. Membr. Sci*., **447**, 73 (2013).
11. H. Cong, M. Radosz, B. F. Towler and Y. Shen, *Sep. Purif. Technol*., **55**, 281 (2007).
12. Y. Kong, H. Du, J. Yang, D. Shi, Y. Wang, Y. Zhang and W. Xin, *Desalination*, **146**, 49 (2002).
13. S. S. Hosseini, Y. Li, T. S. Chung and Y. Liu, *J. Membr. Sci*., **302**, 207 (2007).
14. M. Sadeghi, G. Khanbabaei, A. H. Saeedi Dehaghani, M. Sadeghi, M. A. Aravand, M. Akbarzade and S. Khatti, *J. Membr. Sci*., **322**, 423 (2008).
15. J. Ahn, W. Chung, I. Pinnau and M. D. Guiver, *J. Membr. Sci*., **314**, 123 (2008).
16. M. Sadeghi, M. A. Semsarzadeh, M. Barikani and M. Pourafshari Chenar, *J. Membr. Sci*., **376**, 188 (2011).
17. D. G. Pye, H. H. Hoehn and M. Panar, *J. Appl. Polym. Sci*., **20**, 1921 (1976).
18. M. Naghsh, M. Sadeghi, Moheb A, Pourafshari Chenar M and M. Mohagheghian, *J. Membr. Sci.*, **423**, 97 (2012).
19. S. M. Park, Y. W. Choi, T. H. Yang, J. S. Park and S. H. Kim, *Korean J. Chem. Eng*., **30**, 87 (2013).
20. K. C. O'Brien, W. J. Koros, T. A. Barbari and E. S. Sanders, *J. Membr. Sci*., **29**, 229 (1986).
21. D. Q. Vu, W. J. Koros and S. J. Miller, *J. Membr. Sci*., **211**, 311 (2003).
22. M. M. Talakesh, M. Sadeghi, M. Pourafshari Chenar and A. Khosravi, *J. Membr. Sci*., **415**, 469 (2012).
23. E. Kucukpinar and P. Doruker, *Polymer*, **44**, 3607 (2003).
24. N. Hu and J. R. Fried, *Polymer*, **46**, 4330 (2005).
25. I. G. Economou, V. E. Raptis, V. S. Melissas, D. N. Theodorou, J. Petrou and J. H. Petropoulos, *Fluid Phase Equilib*., **228**, 15 (2005).
26. E. Farno, A. Ghadimi, N. Kasiri and T. Mohammadi, *Sep. Purif. Technol*., **81**, 400 (2011).
27. M. Sadeghi, M. M. Talakesh, B. Ghalei and M. R. Shafiei, *J. Membr. Sci*., **427**, 21 (2013).
28. G. Lei, Z. Zhu and V. Rudolph, *Sep. Purif. Technol*., **78**, 76 (2011).
29. M. Pakizeh, A. N. Moghadam, M. R. Omidkhah and M. Namvar-Mahboub, *Korean J. Chem. Eng*., **30**, 751 (2013).
30. J. Albo, H. Hagiwara, H. Yanagishita, K. Ito and T. Tsuru, *Ind. Eng. Chem. Res*., **53**, 1442 (2014).
31. L. M. Robeson, *J. Membr. Sci*., **320**, 340 (2008).